



## Fine-scale benthic biodiversity patterns inferred from image processing



Jason E. Tanner<sup>a,b,\*</sup>, Camille Mellin<sup>b,c</sup>, Lael Parrott<sup>d</sup>, Corey J.A. Bradshaw<sup>a,b</sup>

<sup>a</sup> South Australian Research and Development Institute – Aquatic Sciences, P.O. Box 120, Henley Beach, South Australia 5022, Australia

<sup>b</sup> The Environment Institute and School of Biological Sciences, The University of Adelaide, Adelaide, South Australia 5005, Australia

<sup>c</sup> Australian Institute of Marine Science, PMB No. 3, Townsville MC, Townsville, Queensland 4810, Australia

<sup>d</sup> Earth & Environmental Sciences and Biology Units, The University of British Columbia, Okanagan Campus, 3333 University Way, Kelowna, BC V1V 1V7, Canada

### ARTICLE INFO

#### Article history:

Received 17 November 2014

Received in revised form 18 February 2015

Accepted 23 February 2015

Available online

#### Keywords:

Evenness

Richness

Mean information gain

Mean mutual information

Spectral signal

Ecological indicator

### ABSTRACT

Despite potentially considerable advantages over traditional sampling techniques, image-derived indices of habitat complexity have rarely been used to predict patterns in marine biodiversity. Advantages include increased speed and coverage of sampling, avoidance of destructive sampling, and substantially reduced processing time compared to traditional taxonomic approaches, thus providing a starting point for more detailed analysis if warranted. In this study, we test the idea that the mean information gain (MIG) and mean mutual information (MMI), two indices of image heterogeneity that we derived from photographs of marine benthic assemblages, represent good preliminary predictors of biodiversity patterns for 133 benthic invertebrate and algal taxa on jetty pylons in Gulf St Vincent, South Australia. Both MIG and MMI were spatially structured, with evidence of among-site differences that were also evident in the benthic data. When combined with information on the spatial structure within the dataset (site and depth), MIG and MMI explained ~35% of deviance in invertebrate species richness, ~43% in Shannon's evenness and up to 50% of dissimilarity in species composition. This explanatory power is of a similar magnitude to many other, less readily available, surrogate measures of biodiversity. These results corroborate the idea that indices of image heterogeneity can provide useful and cost-effective complements to traditional methods used for describing (or predicting) marine epibiota biodiversity patterns. This approach can be applied to many case studies for which photographic data are available, and has the potential to result in substantial time and cost savings.

© 2015 Elsevier B.V. All rights reserved.

## 1. Introduction

The importance of being able to do rapid assessments of marine biodiversity cannot be understated. Today only a little over 2% of the oceans fall under some sort of protection (Moffitt et al., 2015). An inherent assumption of marine conservation planning is that maximizing the representation of species diversity begets higher ecosystem resilience (McCann, 2000; Ives and Carpenter, 2007; Moilanen et al., 2009), because higher species richness and greater niche partitioning lead to weaker biotic interactions, increased

species co-existence and greater functional redundancy (Walker, 1992; Shurin, 2007; Thibaut et al., 2012). Moreover, species richness and niche partitioning tend to be higher in more complex environments (Hutchinson, 1957), leading to the idea that an environment's 'complexity' – measured indirectly as some index of diversity, or more directly based on measures of habitat heterogeneity – can be used as a proxy to predict an ecosystem's resilience to perturbation and environmental change (McCann, 2000; Ives and Carpenter, 2007).

Compared to sampling in terrestrial ecosystems, the relative difficulty, high cost and intensity of sampling marine biota sufficiently to answer ecological and conservation questions (Richardson and Poloczanska, 2008) demands the development of more efficient and meaningful biodiversity approaches and proxies (Mellin et al., 2011, 2012). Combined with difficulties in species identification (including the increasing rarity of specialist taxonomists – Hopkins and Freckleton, 2002), the large number

\* Corresponding author at: South Australian Research and Development Institute – Aquatic Sciences, P.O. Box 120, Henley Beach, South Australia 5022, Australia. Tel.: +61 8 8207 5489.

E-mail addresses: [jason.tanner@sa.gov.au](mailto:jason.tanner@sa.gov.au) (J.E. Tanner), [camille.mellin@adeaide.edu.au](mailto:camille.mellin@adeaide.edu.au) (C. Mellin), [lael.parrott@ubc.ca](mailto:lael.parrott@ubc.ca) (L. Parrott), [corey.bradshaw@adelaide.edu.au](mailto:corey.bradshaw@adelaide.edu.au) (Corey J.A. Bradshaw).

of undescribed marine species, and the variable success of using 'surrogates' (Rodrigues and Brooks, 2007) to infer marine biodiversity distributions (Poore and Wilson, 1993; Ward et al., 1999; Beger et al., 2003; Mellin et al., 2011), simple, efficient and cost-effective methods for assessing plot-based biodiversity are surprisingly rare in marine science.

One particularly promising avenue of methodological development to combat these difficulties is in the application and analysis of video and still photographic images. Baited and unbaited underwater video cameras have been used for some time, and to great effect, to estimate fish abundance and diversity (e.g. Watson et al., 2005; Harvey et al., 2007; Field et al., 2009). While still photographs have been used for over half a century (e.g. Connell et al., 2004), they have traditionally been analysed manually, with individual species identified by relevant taxonomic experts. The automated analysis of still photographs of marine habitats and biota at various scales has only recently been recognised as a potentially efficient biodiversity assessment tool (Mellin et al., 2012; Lambert et al., 2013).

Automated or semi-automated image analysis of still photographs in the context of biodiversity assessment relies on the following assumptions: (i) that structurally complex environments provide, on average, more niches for species (Huston, 1979; Levin, 1999; Bolam et al., 2002), such that direct measurements of species richness (including its variants) should be higher in more spatially complex sampling units; (ii) that for any given spatial scale, structural complexity is by definition greater when the species present are arranged in more spatially complex patterns than in simple patterns (so for example, a chess board is more complex than a board with one half painted white, and the other half painted black); (iii) that two-dimensional photographic images can capture this structural complexity (Proulx and Parrott, 2008, 2009) such that (iv) simple metrics of image heterogeneity are positively correlated with the biodiversity present at the sampling site (Mellin et al., 2012). While the first assumption has been validated using physical descriptors for coral reefs (Luckhurst and Luckhurst, 1978; Friedlander and Parrish, 1998; Attrill et al., 2000), only recently has it been tested using image analysis (Mellin et al., 2012; Lambert et al., 2013). Mellin et al. (2012) found that habitat complexity of coral reefs derived from image analysis at scales of 1–20 km explained up to 29–33% of variation in fish abundance, richness and community structure. Lambert et al. (2013) applied the approach to images of the seafloor substrate at finer spatial scales (0.14 m<sup>2</sup>), and concluded that it was not as effective at predicting epifaunal density as laser line techniques used to measure sea floor rugosity. Earlier work in freshwater lakes showed that a simpler technique, optical intensity, provided an index that was highly correlated to rugosity, and that it was a good predictor of fish richness, diversity and abundance at a scale of 25 m<sup>2</sup> (Shumway et al., 2007). These techniques have also been applied successfully in a variety of terrestrial systems (St-Louis et al., 2006; Bellis et al., 2008; Estes et al., 2008; Proulx and Parrott, 2008, 2009; Oldeland et al., 2010).

Here, we examine the potential of the automated image analysis techniques described by Mellin et al. (2012) and Lambert et al. (2013) to assess the relationship between habitat complexity and benthic epibiota richness and evenness at small spatial scales (0.04 m<sup>2</sup>). While the previous studies examined the relationship between habitat complexity and the diversity and/or abundance of species not necessarily in the image, here we examine the relationship between image heterogeneity and the diversity of species that are present in the image. The ultimate goal is to establish an automated technique for image analysis that provides a reliable preliminary index of marine epibiota biodiversity without the need for comprehensive and time-consuming manual data extraction and species identification typical of processing

images of marine benthos. Instead, the method automatically computes metrics describing the heterogeneity (texture) of the entire image for each of its colour components, and uses these as a multivariate index of image, and by proxy habitat, complexity. If reliable, such a technique would be particularly valuable for monitoring benthic epibiota, for example as part of an impact assessment study or for performance assessment of marine protected areas. A particular advantage is that it could be used to provide a rapid initial assessment of changes in biodiversity, which if detected, could be followed up by more time-consuming, traditional analysis of the photographs to determine in more detail what changes have occurred, and to ensure that putative changes are real and not related to changes in environmental conditions that influence the image but not the assemblage (e.g., light availability at the time of the survey).

## 2. Materials and methods

### 2.1. Study area and data collection

As part of the Transects for Environmental Monitoring and Decision Making network (TREND; [www.trends.a.org.au](http://www.trends.a.org.au)), we photographically examined spatial and temporal variation in benthic assemblages on jetty pylons at five locations (Rapid Bay, Outer Harbour [Adelaide], Ardrossan, Klein Point and Stenhouse Bay) in Gulf St Vincent, South Australia (Fig. 1). Here we use the images from one survey as a case study for the use of image derived indices to predict biodiversity. We chose locations where jetty pylons extended to a sufficient depth ( $\geq 7$  m at lowest astronomical tide) on which we could establish sampling quadrats at three depths:  $\sim 2$ , 4 and 6 m at lowest astronomical tide. At Stenhouse Bay, Klein Point and Outer Harbour, we surveyed only a single site, whereas at Rapid Bay and Ardrossan, the jetty structure allowed us to survey two separate sites, each site being an individual dolphin (group of pylons), thus allowing an examination of within-jetty variation. We chose 10 pylons at each site on which we set 20 cm  $\times$  20 cm sampling quadrats (with one quadrat per pylon and depth level, i.e., 30 quadrats/site). Pylons were mostly square or I-shaped of approximately 25 cm  $\times$  25 cm dimensions, but with round pylons of approximately 30-cm radius at Klein Point.

For all quadrats at each site we took photographs (Fig. 2) with a Panasonic Lumix (DMC-FT2) digital camera set on auto and Inon UWL100-28AD lens, using a frame that ensured they were taken from an equal distance (28 cm) from the pylon and with 2 Inon D180 strobes attached at fixed distances and angles. All photographs were taken in February 2012. Of the 210 quadrats photographed, 12 images at Outer Harbour and 1 at Klein Point were of poor quality due to high turbidity, and  $< 50\%$  of randomly selected points (see below) within the image could be assigned to a taxon. We deleted these photographs from the dataset. For the remaining 197 photographs, we calculated percent cover only on the points that could be assigned to a taxon (there was no bare substratum in any of these plots).

We subsequently cropped each photograph to retain only the area inside the quadrat frame, and then analysed them using two different techniques. First, a benthic invertebrate specialist scored them, with the aid of an algal specialist, to determine percent cover of all taxa present from 50 stratified random points per image using the software package photoQuad (Trygonis and Sini, 2012). While some taxa could be unambiguously identified to species from the photographs (with the aid of specimen collections), most could only be identified to genus, and some to higher levels such as family (see Supplementary Table A1 for a full list of taxa). To retain maximum information in the analysis, taxa were analysed at the lowest common level at which they could be identified (i.e., they were not pooled to the lowest common level of phylum). Secondly,

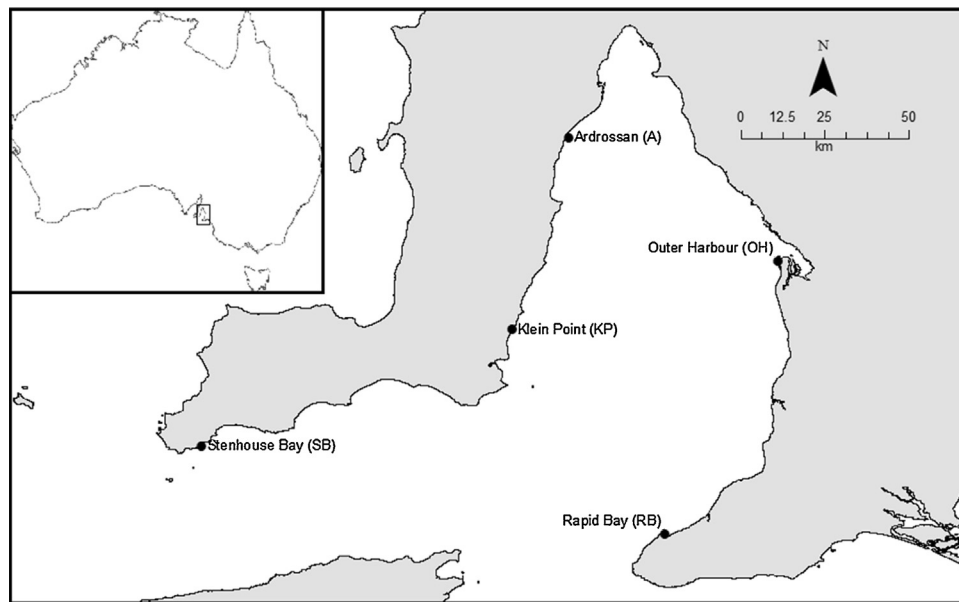


**Fig. 1.** Map of Gulf St Vincent, South Australia showing positions of the five study locations. Inset, map of Australia with study area boxed.

they were subjected to automated image analysis as described below.

## 2.2. Image treatment

We resized each image to 1275 pixels  $\times$  1275 pixels (i.e., the pixel dimensions of the smallest image) to ensure all images were comparable. We then converted images from RGB (red, green, blue) to HSV (hue, saturation and value), a colour model that is preferred for image processing purposes since it decouples

intensity from colour-carrying information (hue and saturation), providing a more intuitive description of colour (Gonzalez and Woods, 2008). This separation also permits an analysis of the degree to which colour specifically contributes to habitat complexity. Each image was therefore encoded by a matrix of dimensions 1275 pixels  $\times$  1275 pixels  $\times$  3 colour components.

For each of the three colour components (i.e., H, S, & V) in each image, we calculated two measures of heterogeneity: (i) mean information gain (MIG; also known as ‘Kullback-Leibler divergence’) (Wackerbauer et al., 1994; Andrienko et al., 2000), and

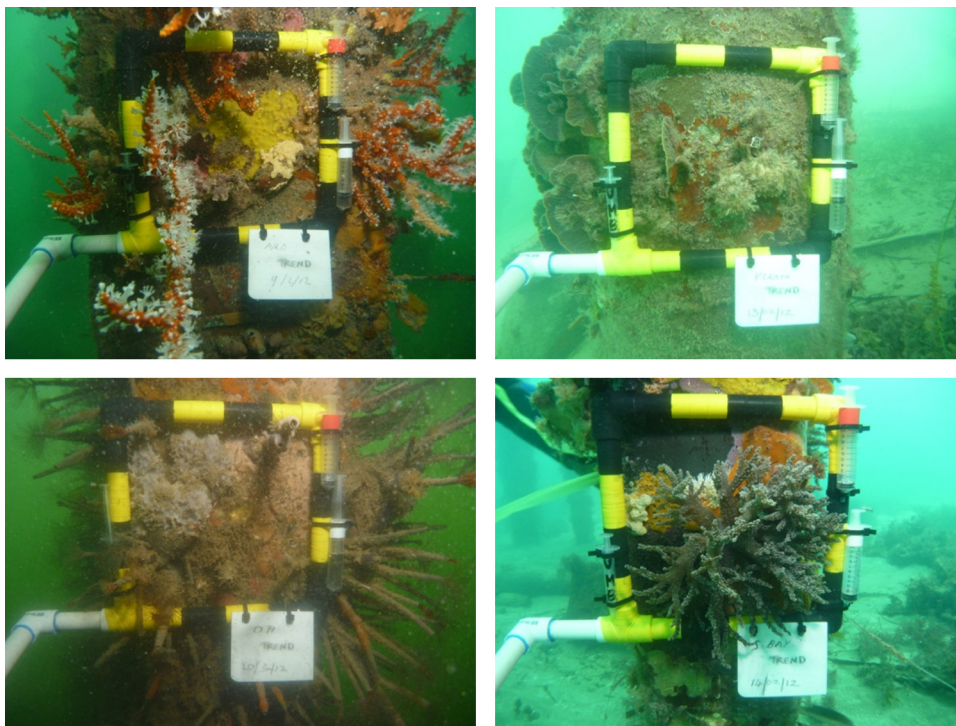


**Fig. 2.** Representative images of quadrat photos taken at the jetty pylons. We used only the area inside the quadrat (20 cm  $\times$  20 cm) for analysis, with the image further cropped to the pylon extent if necessary. Upper left: Ardrossan (dolphin 1); upper right: Klein Point; lower left: Outer Harbour; lower right: Stenhouse Bay.

(ii) fourth-order mean mutual information (MMI). MIG is a measure of disorder and quantifies the spatial heterogeneity of an image, with values ranging from 0 for a completely solid-colour image to 1 for a uniformly random image, and heterogeneous images having intermediate MIG values (Mellin et al., 2012). The MIG index for each colour component in an image is calculated as:

$$\text{MIG} = \frac{-\sum_{j=1}^{M^k} p(\chi_j) \log p(\chi_j) + \sum_{i=1}^M p(\gamma_i) \log p(\gamma_i)}{\log(M^k/M)}$$

where  $p(\gamma_i)$  is the relative frequency of pixel value  $\gamma_i$  in the image and  $p(\chi_j)$  is the relative frequency with which a specific spatial configuration  $\chi_j$  of  $k$  values is observed. For  $M$  classes of values, the number of possible configurations in a  $k$ -pixel neighbourhood is  $M^k$  (Proulx and Parrott, 2009).

MMI indicates the presence of spatial structure in the image and ranges from 0 for random patterns to 1 for uniform ones (Wackerbauer et al., 1994; Proulx and Parrott, 2008). MMI is calculated as:

$$\text{MMI} = \frac{-4 \sum_{i=1}^M p(\gamma_i) \log p(\gamma_i) + \sum_{j=1}^{M^k} p(\chi_j) \log p(\chi_j)}{4 \log(M^k/M)}$$

While in theory these measures could be calculated for images having pixel values  $\gamma_i$  over any range (e.g., integers ranging from 0 to 255 for RGB images, continuous values between 0 and 1 for hue and saturation), doing so would be computationally intractable and lead to errors due to undersampling in images of only a few thousand pixels (i.e., many spatial configurations  $\chi_j$  would not be adequately represented). To avoid biases due to undersampling, the ratio of the total number of pixels in an image to  $M^k$  should not be  $<100$  (Mellin et al., 2012). For this reason, pixel values need to be re-classified into a smaller range of values and the size of the spatial neighbourhood ( $k$ ) that can be considered is limited. For image sizes of 1275 pixels  $\times$  1275 pixels, and  $k = 4$  (i.e., a block of 2 pixels  $\times$  2 pixels), a maximum of  $M = 11$  colour classes is possible. Increasing the spatial neighbourhood to  $k = 9$  (i.e., a block of 3 pixels  $\times$  3 pixels) decreases the number of possible colour classes to 2 or 3 to ensure adequate representation of all possible spatial configurations ( $M = 2.9$  to respect the above-mentioned ratio). Given the large textural information lost in converting the colour bands to only 2 or 3 values, and considering the probable importance of colour and texture in determining habitat complexity of shallow marine environments, we chose to maximise the number of colour classes used in our analyses. We thus chose to use  $k = 4$  and  $M = 10$  (while  $M = 11$  was theoretically possible, we chose  $M = 10$  to be certain to avoid any biases and to also be consistent with Proulx and Parrott (2008) and Mellin et al. (2012)). We assigned each pixel value in the images an integer value in the range 1–10 based on its classification into one of  $M = 10$  evenly distributed classes. All image analyses have thus been done for pixel values,  $\gamma_i$  ranging from 1 to 10.

While both MIG and MMI are different measures of Shannon entropies (Proulx and Parrott, 2008), they are neither identical nor highly correlated. While there is some correlation between MIG and MMI for hue at low values, for saturation and value they are uncorrelated (Supplementary Fig. A1). Together, these two sets of indices enable the detection of heterogeneous (i.e., neither random nor completely ordered) (*sensu* Parrott, 2010) spatial patterns in images corresponding to highly complex natural habitats. Matlab code to calculate MIG and MMI is available for download from <http://complexity.ok.ubc.ca/projects/measuring-complexity>.

## 2.3. Analysis

The analysis followed three main steps. First, we assessed the variation in image indices among sites and depth levels. Second, we modelled standard univariate biodiversity indices (i.e., benthic taxonomic richness and evenness in taxon abundances) as a function of image indices. Last, we modelled multivariate biodiversity indices (matrix of benthic taxa percent coverage) as a function of image indices, accounting for the spatial structure in the data.

### 2.3.1. Image indices

We first assessed the extent to which image indices (MIG and MMI of the hue, saturation and value) varied among sites and depth levels, these indices being considered both (i) separately and (ii) collectively. We achieved this by using (i) generalised mixed-effects linear models (GLMM) of each image index (e.g., MIG of the hue) with random effects *Site*, or *Depth* nested within *Site*, to test which spatial structure best represented the data; and (ii) a multivariate analysis of variance (based on distance matrices and 1000 permutations; PERMANOVA) (Anderson, 2001) of the entire matrix of image indices (MIG and MMI of the hue, saturation and value), with *Site* and *Depth* as predictors. *Depth* was accounted for as a three-level factor (i.e., upper  $\sim 2$  m; mid  $\sim 4$  m; deeper  $\sim 6$  m below lowest astronomical tide).

All image indices were bounded by 0 and 1, so we used a binomial error distribution with a logit link in the GLMM. Although the binomial error distribution is more commonly applied to counts of successes and failures (or the ratio between them), it can also be the most appropriate error distribution for ecological indices bounded by 0 and 1 (Mellin et al., 2014). This assumption was validated by the normal distribution of model residuals assessed using normalised scores of standardised residual deviance (Q–Q plots). We evaluated model support using Akaike's information criterion corrected for small sample sizes ( $AIC_c$ ) and corresponding weights ( $wAIC_c$ ) that assign relative strengths of evidence to the different competing models (Burnham and Anderson, 2002, 2004). We also used the percent deviance explained in the response variable (*De*) as a measure of the model's goodness-of-fit, calculated as the difference between each model's deviance and that of the null (intercept only) model, multiplied by 100 and divided by the null deviance.

### 2.3.2. Univariate biodiversity indices

We modelled two univariate indices of benthic biodiversity from the benthic percent cover matrix for each individual image: taxonomic richness (denoted as *R* here to avoid confusion with image saturation [*S*]), defined as the total number of taxa recorded in each quadrat (i.e., the number of taxa when identified to the most precise taxonomic level possible; not necessarily to species), and Shannon's evenness index (denoted as *E* here to avoid confusion with image hue [*H*]) as a measure of evenness in taxon abundances within each quadrat (Krebs, 1999). Also known as 'equitability', Shannon's evenness index describes the distribution of abundances of all taxa, with a totally 'even' community being one with equal abundances of all species represented.

We predicted *R* and *E* as a function of image indices using two sets of random-intercept, fixed-slope, Poisson error-distributed GLMM with *Site* as a random effect to account for the non-independence of quadrats within the same site. We also included *Depth* as a fixed effect; including it as an additional random effect resulted in no improvement in model performance based on  $wAIC_c$  (Supplementary Table A2). The models used are of the form:

$$S \sim a + \beta_h \text{MIG.H} + \beta_s \text{MIG.S} + \beta_v \text{MIG.V} + \beta_d \text{Depth} + \beta_{si} (1|\text{Site}) + \epsilon$$

For each response variable (*R* or *E*), the final model set consisted of (i) MIG indices, *Depth* (fixed) and *Site* (random), (ii) MMI indices,

*Depth* (fixed) and *Site* (random), (iii) both MIG and MMI indices, *Depth* (fixed) and *Site* (random), (iv) *Depth* and *Site* (spatial structure) only and (v) the null (intercept-only) model. To assess potential nonlinear relationships between image indices and *R* or *E*, we considered both linear and quadratic terms for each image index (e.g., MIG of the hue) in the models. We did not consider other combinations of MIG and MMI indices in the final model set because a preliminary model set showed that they received no support (i.e., negligible Akaike weights based on  $AIC_c$ , i.e.,  $wAIC_c < 0.001$ ).

We assessed the predictive ability of the top-ranked model according to  $AIC_c$  using a 10-fold cross-validation (Davison and Hinkley, 1997). This bootstrap resampling procedure (here using 1000 iterations) estimates the mean model prediction error for 10% of observations randomly omitted from the calibration dataset.

### 2.3.3. Multivariate biodiversity indices

We partitioned the variation in the benthic percent cover matrix explained by image indices (MIG and MMI) and by the spatial structure (*Depth* within *Site*) using a constrained distance-based redundancy analysis with 1000 permutations (Legendre and Anderson, 1999). To achieve this, we computed a Bray–Curtis distance matrix based on the benthic cover matrix and a Euclidian distance matrix based on image indices (i.e., including both MIG and MMI indices). Successively constraining each source of variation (i.e., image indices or spatial structure) on the others allowed us to estimate the proportion of variance explained by each source exclusively as well as shared proportions.

To estimate the correlation between image indices and multivariate indices of benthic diversity, we did a Mantel correlation test between benthic and image indices' distance matrices based on 1000 permutations. We used Bray–Curtis distance for benthic cover and Euclidean distance for image indices; both were calculated using the *vegdist* function of the *vegan* package (Oksanen et al., 2013) in R (R Core Team, 2013).

To visualise the correlation between the ordination of sites based on benthic composition and that based on image indices, we did a non-metric multidimensional scaling based on these two matrices, followed by a Procrustes rotation of the image MDS based on the benthic one to make them readily comparable (Peres-Neto and Jackson, 2001). Finally, we did a Procrustes test of the correlation between the two resulting configurations (Peres-Neto and Jackson, 2001).

## 3. Results

### 3.1. General biodiversity patterns

The invertebrate assemblages present on the jetty pylons at each site were diverse, with between 33 and 60 taxa present in the 30 quadrats at each site, and an average of  $6.44 \pm 0.18$  (SE) taxa per quadrat. We identified 133 taxa in total across all five jetties, 112 invertebrates and 21 algae (Supplementary Table A1). Assemblage composition was highly variable among sites, and even between dolphins only 10–20 m apart (Fig. 3). At Ardrossan, one dolphin was dominated by anthozoans, primarily the soft coral *Carijoa* sp. and the hard coral *Culicea* sp. ( $55.1 \pm 4.3\%$ ), whereas the other was dominated by unidentified rhodophyta (red algae,  $63.6 \pm 3.1\%$ ). Klein Point was also dominated by rhodophyta, being primarily a mix of *Laurencia* sp. and unidentified species ( $56.6 \pm 6.1\%$ ). The other sites were less dominated by a single group, although in all cases one group of organisms exceeded 30% cover (Outer Harbour – polychaete worms, entirely the invasive *Sabella spallanzanii*; Rapid Bay and Stenhouse Bay – anthozoa, primarily the scleractinian coral *Culicea* sp. at the former and the soft coral *Drifa gaboensis* at the latter). Species abundance distribution curves based

on individual taxa showed a similarly strong pattern of dominance by a few individual taxa at each site (Supplementary Fig. A2). For six of the seven sites, two taxa accounted for >50% of the cover, with the exception being Rapid Bay 2, where the two most dominant taxa accounted for 49%. There was then a long tail of increasingly rare taxa. An unidentified rhodophyte and *Culicea* sp. had the broadest distribution, occurring in 109 and 104 of the 197 quadrats, respectively, and were the only two taxa with >10% cover when averaged across all sites (Supplementary Table A1).

### 3.2. Spectral signal-biodiversity relationships

We found evidence for an effect of *Site* on all image indices (Supplementary Table A2), explaining up to 25% of deviance in the MIG of the hue (MIG\_H). This suggests that the deviance in MIG most likely arises from variation in colour among taxa and not just variation in light intensity among depths, sites or sampling times. When all image indices were considered collectively, *Site* explained 43% of the variation in the image index matrix ( $P < 0.001$ ; PERMANOVA; 1000 permutations).

Benthic taxon richness (*R*) and Shannon's evenness (*E*) differed among *Site* levels, and among *Depth* levels to a lesser extent (Fig. 4). *Site* (random) and *Depth* (fixed) explained 14% of deviance in *R* and 6% of deviance in *E* (Table 1). Adding MIG and MMI indices as fixed effects in the models resulted in an increase of the deviance explained to 34.5% for *R* and 43.1% for *E*. Including the location (to account for variable number of sites; i.e., dolphins, in each location) did not result in any model improvement (Supplementary Table A3), so we only kept *Site* as a random effect in the final models. The top-ranked models resulted in a mean cross-validated prediction error of 24% for *R* and 28% for *E*; residuals were normally distributed and predictions explained 34 and 36% of variation in observations of *R* and *E*, respectively (Supplementary Fig. A3).

Distance matrices based on image indices and on benthic composition were correlated (Spearman's  $\rho = 0.26$ ;  $P < 0.001$ ; 1000 permutations). Partitioning the variation in the benthic cover matrix resulted in 25% of variation explained by image indices (within-image spatial structure), most of which was also reflected by the between-image spatial structure (i.e., *Site* and *Depth*, Fig. 5). Another 24% was explained by the between-image spatial structure only (i.e., conditioned on the image indices), resulting in 49% attributed to the spatial structure in total, while 51% of variation remained unexplained (residuals). The MDS based on the benthic composition showed a similar site configuration to that given by the Procrustes-rotated MDS based on image indices, although image indices poorly captured the singularity of Rapid Bay quadrats (Fig. 6). The two configurations were strongly correlated (Procrustes correlation test,  $r = 0.47$ ,  $P < 0.001$ ).

## 4. Discussion

Our study adds to the small but growing body of evidence that image analysis can provide reasonable proxies for quantifying at least some components of marine biodiversity patterns 'at a glance', regardless of spatial scale (Andréfouët et al., 2010; Mellin et al., 2012). Indeed, after accounting for spatial non-independence of the sampling sites, we could effectively explain ~35% of the variation in identified taxon richness, over 43% in taxonomic evenness, and up to ~50% in taxon dissimilarity, which are comparable to the variances explained in reef fish biodiversity by image analysis at broader scales in the Great Barrier Reef (Mellin et al., 2012). This also compares favourably to other studies using surrogate measures for biodiversity. For example, Huang et al. (2012) found a wide range of traditional surrogates to explain between 32 and 79% of the variation in a range of diversity metrics and infauna species abundances, while Przesławski et al. (2011)

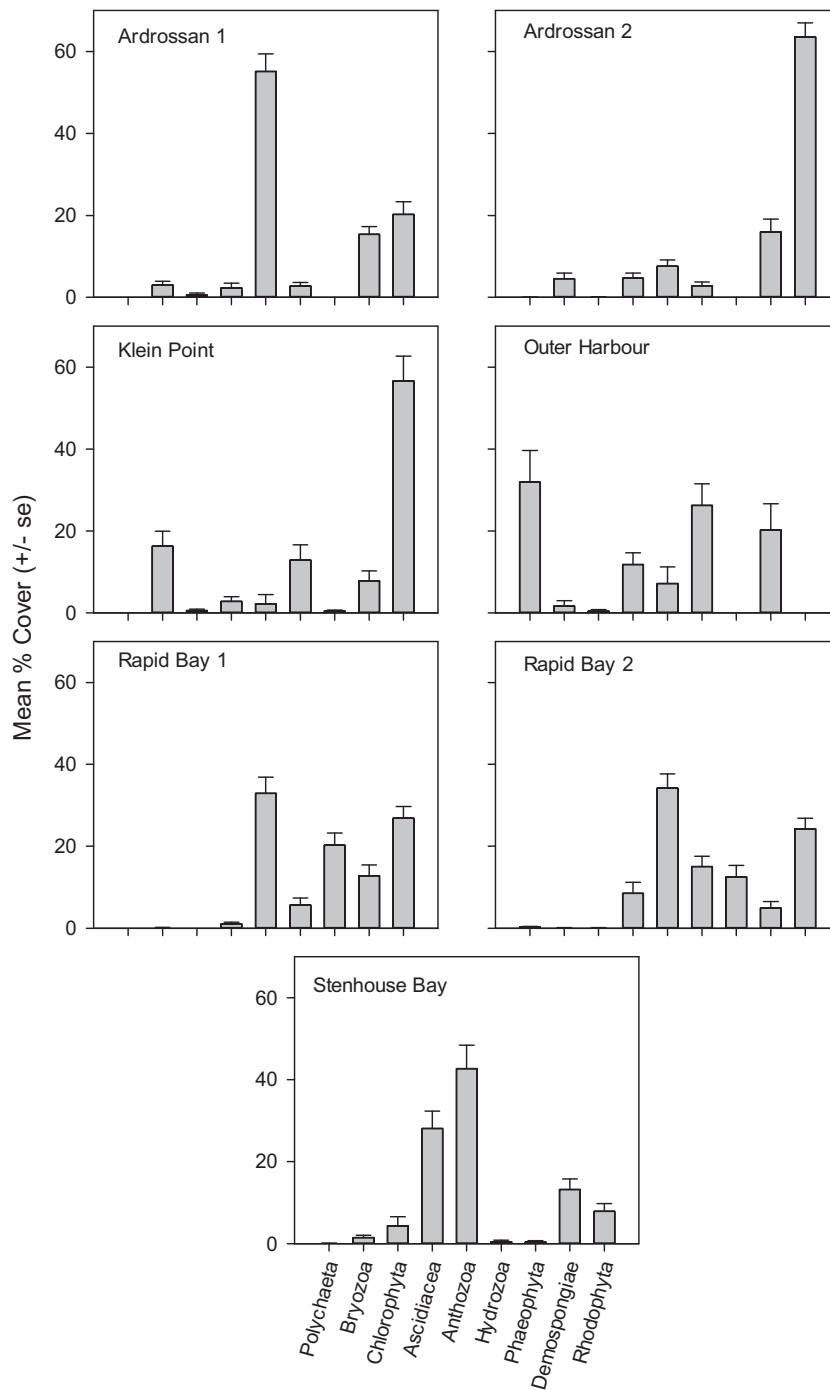


**Fig. 3.** Percentage cover frequency histograms for major taxonomic groups represented on quadrats. For clarity, echinodermata, mollusca and calcarea, each of which occupy <0.5% of the substratum at all sites, are not plotted.

showed that benthic invertebrate community structure was related to habitat characteristics with ANOSIM R statistic ranging from 0.31 to 0.42.

While there is obviously no replacement for physical sampling and detailed species identification using either traditional taxonomy or genetic barcoding, the advantage of quick-assessment photographic proxies is obvious. Not only is the level of expertise required low, thus making it an ideal application for less-experienced students or technicians, the ease and cost efficiency of collecting and analysing digital photographs will suit a wide variety of marine applications. These could include inter alia assessments of marine protected areas, invasive species

monitoring, disturbance impacts (e.g., before–after/control–impact experiments), and general biodiversity monitoring studies. Indeed, many such studies already rely partly or fully on photographic data collection, and thus the field component would not need to change. For this study, processing of the images and identification by a taxonomic expert took some 30–40 min per image. In comparison, processing of the images and calculation of MIG and MMI only required 1–2 min per image, representing a saving of 100+ hours for the 197 images analysed here. In a companion project, ~1500 images are available, and the potential saving of 750+ hours represents 20 weeks full-time work by someone with good taxonomic skills. As with any technique,

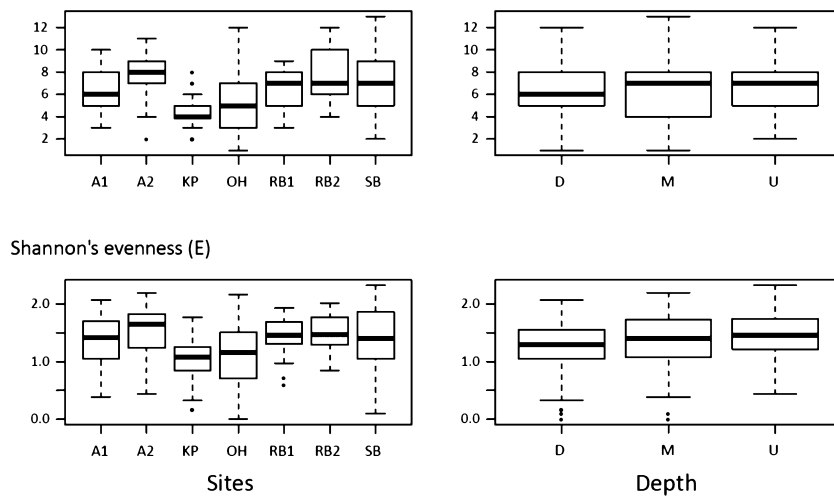


**Fig. 4.** Boxplots of taxonomic richness ( $R$ , upper panels) and Shannon's evenness index ( $E$ , lower panels) among sites (see abbreviations in Fig. 1) and depths (U, upper ~2 m; M, mid ~4 m; D, deeper ~6 m below lowest astronomical tide). Shown are the median (thicker line), lower and upper quartiles (box boundaries), 10 and 90% percentiles (whiskers) and outliers (dots).

however, the utility of these image indices needs to be confirmed for each individual application before they are broadly applied. Further, many of our sample quadrats were dominated by only a few taxa – a phenomenon likely characteristic of many fine-scale assessments – yet the predictive performance was still remarkably high. In other words, the technique should be effective in both species-rich and species-poor environments.

The indices of complexity we used here detect spatial heterogeneity in the photographed scene. The analyses are based on the assumption that increased taxonomic diversity increases image heterogeneity, producing patterns of colour and texture in the photograph that are neither random nor uniform (Proulx and Parrott, 2008). Indeed, it is logical to suppose that a more diverse benthic epibiota community should present a wider variety of

shapes and colours and that this variety would be detectable in an image. Complexity, however, goes further than this, and also incorporates the spatial arrangement of the species present. For example, two plots each with 50% cover of species A and 50% cover of species B have the same species richness and evenness. However, if one plot has a single colony of each, while the other plot has 20 intermingled colonies, they will have greatly different complexity, and potentially different responses to perturbations. This within-plot spatial heterogeneity will account for an unknown proportion of the unexplained variance that we document. However, rather than being extraneous noise, this heterogeneity is actually an important part of the signal, as more complex ecological systems tend to be more resilient (McCann, 2000; Ives and Carpenter, 2007). Such simple measures of complexity like those we used provide promising avenues for rapidly assessing and monitoring the states of a wide range of ecosystem types (Parrott, 2010).

Image heterogeneity will also be influenced by the species abundance distribution (Supplementary Fig. A2), with images dominated by a single species likely to be more homogenous than an image with the same number of species but a more even distribution. Thus we were able to explain more variation in taxonomic evenness (43%) than richness (35%). Oldeland et al. (2010) found a similar result for terrestrial vegetation, ascribing it to the fact that evenness better matches vegetation structure, which is a component of habitat heterogeneity. Similarly, Foody and Cutler (2003) and Dogan and Dogan (2006) found that image analysis explained a greater proportion of the variation in evenness than richness, although the difference tended to be small, suggesting that this may be a general trend.

Methodological issues related to the size and resolution of photographic images we used need to be considered when calculating MIG and MMI. For comparative purposes, all images need to be the same number of pixels in size and should represent the same spatial extent. As for any spatial analysis, decreasing the resolution (i.e., increasing the grain) of an image increases the size of the smallest spatial structures that can be detected. Since habitat complexity is likely scale-dependent, substantially decreasing image resolution can affect results by reducing the ability of the algorithms to detect fine-scale heterogeneity in the photographed scene. Ultimately, the choice of spatial extent and resolution defines the scales of structures that can be studied in an image. The number of photographs also needs to be carefully considered.

**Table 1**

Final generalised linear mixed-effects model (GLMM) results for species richness ( $R$ ) and Shannon's evenness index ( $E$ ) as a function of mean information gain (MIG) and mean mutual information (MMI) indices of image heterogeneity (both include image hue, saturation and value, so for example  $MIG = MIG\_H + MIG\_S + MIG\_V$ ), site and depth.  $MIG^2$  (or  $MMI^2$ ) indicates that quadratic terms of MIG (or MMI) indices are included in addition to linear terms. All models include spatial structure among sites as the random effect (excluding the intercept-only null model). Shown are the estimated number of model parameters ( $j$ ), maximum log-likelihood, the information-theoretic Akaike's information criterion corrected for small samples ( $AIC_c$ ),  $AIC_c$  weight ( $wAIC_c = \text{model probability}$ ) and the percent deviance explained ( $De$ ) as a measure of the model's goodness-of-fit. Models are ordered by decreasing  $wAIC_c$ .

Model	$j$	$LL$	$AIC_c$	$wAIC_c$	$De$
$R \sim MIG + MMI + \text{Depth} + (1 \text{Site})$	11	-63.79	151.01	0.795	34.46
$R \sim MIG^2 + MMI^2 + \text{Depth} + (1 \text{Site})$	17	-58.16	153.74	0.203	40.24
$R \sim MMI^2 + \text{Depth} + (1 \text{Site})$	11	-69.73	162.89	0.002	28.35
$R \sim MIG^2 + \text{Depth} + (1 \text{Site})$	11	-72.39	168.22	<0.001	25.61
$R \sim MMI + \text{Depth} + (1 \text{Site})$	8	-78.00	172.76	<0.001	19.86
$R \sim MIG + \text{Depth} + (1 \text{Site})$	8	-78.88	174.53	<0.001	18.95
$R \sim \text{Depth} + (1 \text{Site})$	5	-83.73	177.78	<0.001	13.97
$R \sim 1 + (1 \text{Null\_RE})$	3	-97.32	200.77	<0.001	-
$E \sim MIG^2 + MMI^2 + \text{Depth} + (1 \text{Site})$	17	-73.92	185.25	1.000	43.10
$E \sim MMI^2 + \text{Depth} + (1 \text{Site})$	11	-98.04	219.51	<0.001	24.52
$E \sim MIG + MMI + \text{Depth} + (1 \text{Site})$	11	-99.90	223.22	<0.001	23.10
$E \sim MIG^2 + \text{Depth} + (1 \text{Site})$	11	-100.26	223.94	<0.001	22.82
$E \sim MIG + \text{Depth} + (1 \text{Site})$	8	-115.26	247.29	<0.001	11.27
$E \sim MMI + \text{Depth} + (1 \text{Site})$	8	-115.81	248.38	<0.001	10.85
$E \sim \text{Depth} + (1 \text{Site})$	5	-122.23	254.77	<0.001	5.90
$E \sim 1 + (1 \text{Null\_RE})$	3	-129.90	265.92	<0.001	-

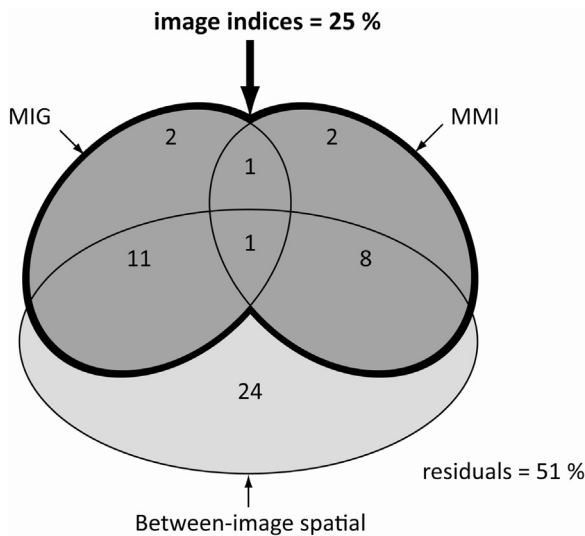


**Fig. 5.** Venn diagram of variation in the benthic cover matrix partitioned among fixed effects from redundancy analysis models. Numbers given are percent variation in the benthic cover matrix. The dark envelope represents the total variation explained by indices of image heterogeneity (mean information gain [MIG] and mean mutual information [MMI]). *Between-image spatial* refers to the *Depth within Site* spatial structure.

While we have used a relatively low number of images (197) compared to what are often available, further decreases in sample size would likely result in model over-parameterisation, and the need to focus on simpler models. Whether these models would then be able to capture a meaningful proportion of the deviance in the data would have to be determined.

Another advantage of spectral analysis is that it does not preclude more detailed analysis of the photographic images later if the initial findings show a pattern of interest. The photographs can still be used for more traditional approaches such as determining percent cover of different taxa, and with the rapidly increasing resolution of digital cameras, the taxonomic resolution achievable is now reaching species level in some higher taxa (e.g., scleractinian corals, Tanner, pers. obs.). While many of the taxa recorded here could not be identified to species, we are confident that most would either be a single species, or a cluster of cryptic

species. It is unlikely that better taxonomic resolution could have been achieved via time consuming in situ identification, and assigning the taxa identified here to species would require collection of specimens and detailed laboratory work by an expert taxonomist. Given the long tail of rare taxa present (Supplementary Fig. A2), to collect all of them for laboratory identification would require either sacrificing the survey plots, or sacrificing a much larger area adjacent to them. The former would preclude any form of repeated sampling, while the latter could influence the target assemblage due to extensive manipulation and destruction of surrounding organisms. There is also increasing pressure from managers to move to non-destructive sampling, especially in marine parks, making it necessary to extend the suite of tools available for photo-analysis. An increasing number of studies have examined the issue of taxonomic sufficiency for marine benthos, and have shown that diversity at the genus and/or family level is generally a good predictor of diversity at the species level (e.g., Hirst, 2008; Bevilacqua et al., 2012), and hence in terms of examining patterns of biodiversity, it is not particularly important to identify the taxa present to species level.

As awareness of marine conservation is growing, there is increasing research into the use of surrogates to measure patterns in biodiversity (Włodarska-Kowalczyk and Kędra, 2007; Musco et al., 2009; McArthur et al., 2010; Mellin et al., 2011; Smale et al., 2011), and many marine planning decisions are now based on surrogates rather than fully quantifying the assemblage(s) of interest. However, often there is little or no assessment of how well the patterns in these surrogate variables reflect patterns in individual components of biodiversity (Hirst, 2008; Mellin et al., 2011; Kenchington and Hutchings, 2012). That we can capture some 50% of the variation in community composition in simple models using indices from photographs bodes well for the use of this technique as a surrogate for biodiversity.

Our study also advances our previous work at broader scales (Mellin et al., 2012) by demonstrating the utility of incorporating multiple spectral signals into a biodiversity metric, rather than relying on a single spectral signal. In all responses and combinations we considered, the combination of hue, saturation and value in both mean information gain and mean mutual information consistently gave the best predictive results. MIG and MMI are only weakly correlated (Spearman's  $\rho = 0.30$ ), and measure different aspects of image heterogeneity, and so should be considered simultaneously when assessing spectral signal performance.

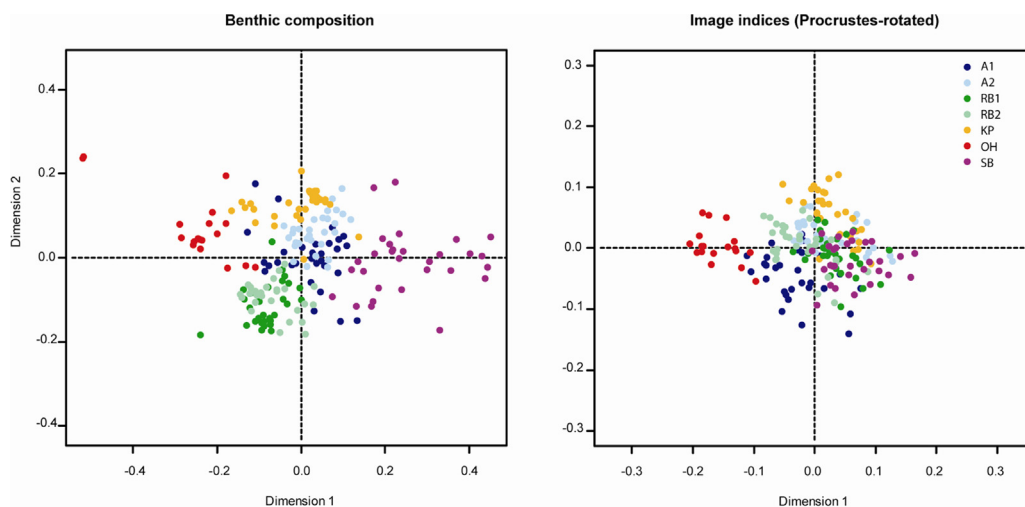


**Fig. 6.** Non-metric multidimensional scaling of the benthic composition matrix (left panel) and the image index matrix (right panel) after a Procrustes rotation of the latter based on the former (see text for details). Colours correspond to sites (see abbreviations in Fig. 1).



Additional work is required to assess the effectiveness of spectral signals for quantifying epibiota biodiversity patterns at all scales, but particularly for fine- and meso (1–100 m) scales. Further, performance needs to be assessed under different light availability, depth, turbidity, temperature and ecotone conditions. Although we sampled three depth levels, these were only 2 m apart and did not result in any differences, either in terms of image complexity or benthic diversity among depths. However, we did factor out the potential effect of (unmeasured) turbidity conditions; indeed, visibility at Outer Harbour (a working port) was only 1–2 m, and at Rapid Bay and Stenhouse Bay it was typically 10–15 m, with both being in more oceanic waters near the mouth of Gulf St Vincent. The influence of topographic complexity that is invariably present in natural substrata also needs to be investigated, as the assemblages surveyed here were growing on flat jetty pylons. This topographic complexity is likely to add heterogeneity to an image, over and above that due to any increases in biodiversity associated with an increase in microhabitat availability, because it will cast different patterns of light and shade on the image. It also remains inconclusive whether such image analysis can be used as diversity proxies for microscopic (e.g., plankton) or mobile (e.g., macroalgae- or seagrass-associated invertebrate) taxa, although measures of habitat are not always a useful surrogate for the latter (Hirst, 2008; Birdsey et al., 2012). This image-analysis approach is also unlikely to be useful for examining infaunal assemblages, because these are structured more by subsurface physical attributes than surface habitat complexity. Nonetheless, the accumulating evidence predicts that it will be useful in many situations, and can be cautiously considered alongside existing techniques in future plans for biodiversity assessment, or applied to archived photos from previous research.

## Acknowledgements

Funded by the South Australia Premier's Science and Research Fund as part of the TRansects for ENvironmental monitoring and Decision making (TREND) network ([www.trendsa.org.au](http://www.trendsa.org.au)). TREND is a collaboration between the University of Adelaide, Primary Industries and Regions South Australia and the South Australian Department of Environment, Water and Natural Resources. The funders played no role in study design, analysis and interpretation of the data, writing, or the decision to publish. We thank A. Dobrovolskis for assistance in the field, and S. Sorokin and K. Wiltshire for photo identifications. CM was supported by the Marine Biodiversity Hub through the Australian Government's National Environmental Research Program (NERP).

## Appendix A. Supplementary data

Supplementary data associated with this article can be found, in the online version, at <http://dx.doi.org/10.1016/j.ecocom.2015.02.009>.

## References

- Anderson, M.J., 2001. A new method for non-parametric multivariate analysis of variance. *Austral Ecol.* 26, 32–46.
- Andréfouët, S., Payri, C., Kulbicki, M., Scopélitis, J., Dalleau, M., Mellin, C., Scamps, M., Dirberg, G., 2010. Mesure, suivi et potentiel économique de la diversité de l'habitat récifo-lagonaire néo-calédonien: inventaire des herbiers, suivi des zones coralliennes et rôle des habitats dans la distribution des ressources en poissons de récifs. In: Rapport Conventions Sciences de la Mer – Biologie Marine No. 31. Institut de Recherche pour le Développement (IRD), Centre de Nouméa/NoûMéa, Nouméa, New Caledonia.
- Andrienko, Y.A., Brilliantov, N.V., Kurths, J., 2000. Complexity of two-dimensional patterns. *Eur. Phys. J. B* 15, 539–546.
- Attrill, M.J., Strong, J.A., Rowden, A.A., 2000. Are macroinvertebrate communities influenced by seagrass structural complexity? *Ecography* 23, 114–121.
- Beger, M., Jones, G.P., Munday, P.L., 2003. Conservation of coral reef biodiversity: a comparison of reserve selection procedures for corals and fishes. *Biol. Conserv.* 111, 53–62.
- Bellis, L.M., Pidgeon, A.M., Radeloff, V.C., St-Louis, V., Navarro, J.L., Martella, M.B., 2008. Modeling habitat suitability for greater rheas based on satellite image texture. *Ecol. Appl.* 18, 1956–1966.
- Bevilacqua, S., Terlizzi, A., Claudet, J., Fraschetti, S., Boero, F., 2012. Taxonomic relatedness does not matter for species surrogacy in the assessment of community responses to environmental drivers. *J. Appl. Ecol.* 49, 357–366.
- Birdsey, E.M., Johnston, E.L., Poore, A.G.B., 2012. Diversity and cover of a sessile animal assemblage does not predict its associated mobile fauna. *Mar. Biol.* 159, 551–560.
- Bolam, S.G., Fernandes, T.F., Huxham, M., 2002. Diversity, biomass, and ecosystem processes in the marine benthos. *Ecol. Monogr.* 72, 599–615.
- Burnham, K.P., Anderson, D.R., 2002. Model Selection and Multimodel Inference: A Practical Information-Theoretic Approach, 2nd edition. Springer-Verlag, New York, USA.
- Burnham, K.P., Anderson, D.R., 2004. Understanding AIC and BIC in model selection. *Sociol. Methods Res.* 33, 261–304.
- Connell, J.H., Hughes, T.P., Wallace, C.C., Tanner, J.E., Harms, K.E., Kerr, A.M., 2004. A long-term study of competition and diversity of corals. *Ecol. Monogr.* 74, 179–210.
- Davison, A.C., Hinkley, D.V., 1997. Bootstrap Methods and Their Application. Cambridge University Press, Cambridge.
- Dogan, H.M., Dogan, M., 2006. A new approach to diversity indices – modeling and mapping plant biodiversity of Nallihan (A3-Ankara/Turkey) forest ecosystem in frame of geographic information systems. *Biodivers. Conserv.* 15, 855–878.
- Estes, L.D., Okin, G.S., Mwangi, A.G., Shugart, H.H., 2008. Habitat selection by a rare forest antelope: a multi-scale approach combining field data and imagery from three sensors. *Remote Sens. Environ.* 112, 2033–2050.
- Field, I.C., Meekan, M.G., Buckworth, R.C., Bradshaw, C.J.A., 2009. Protein mining the world's oceans: Australasia as an example of illegal expansion-and-displacement fishing. *Fish Fish.* 10, 323–328.
- Foody, G.M., Cutler, M.E.J., 2003. Tree biodiversity in protected and logged Bornean tropical rain forests and its measurement by satellite remote sensing. *J. Biogeogr.* 30, 1053–1066.
- Friedlander, A.M., Parrish, J.D., 1998. Habitat characteristics affecting fish assemblages on a Hawaiian coral reef. *J. Exp. Mar. Biol. Ecol.* 224, 1–30.
- Gonzalez, R., Woods, R., 2008. Digital Image Processing, 3rd edition. Pearson Prentice Hall, Upper Saddle River, NJ, USA.
- Harvey, E.S., Cappel, M., Butler, J.J., Hall, N., Kendrick, G.A., 2007. Bait attraction affects the performance of remote underwater video stations in assessment of demersal fish community structure. *Mar. Ecol. Prog. Ser.* 350, 245–254.
- Hirst, A.J., 2008. Surrogate measures for assessing cryptic faunal biodiversity on macroalgal-dominated subtidal reefs. *Biol. Conserv.* 141, 211–220.
- Hopkins, G.W., Freckleton, R.P., 2002. Declines in the numbers of amateur and professional taxonomists: implications for conservation. *Anim. Conserv.* 5, 245–249.
- Huang, Z., McArthur, M., Radke, L., Anderson, T., Nichol, S., Siwabessy, J., Brooke, B., 2012. Developing physical surrogates for benthic biodiversity using co-located samples and regression tree models: a conceptual synthesis for a sandy temperate embayment. *Int. J. Geogr. Inf. Sci.* 26, 2141–2160.
- Huston, M., 1979. General hypothesis of species diversity. *Am. Nat.* 113, 81–101.
- Hutchinson, G.E., 1957. In: Cold Spring Harbor Symposium on Quantitative Biology. (concluding remarks), pp. 415–427.
- Ives, A.R., Carpenter, S.R., 2007. Stability and diversity of ecosystems. *Science* 317, 58–62.
- Kennington, R., Hutchings, P., 2012. Science, biodiversity and Australian management of marine ecosystems. *Ocean Coast. Manag.* 69, 194–199.
- Krebs, C.J., 1999. Ecological Methodology, 2nd edition. Benjamin Cummings, Upper Saddle River, NJ, USA.
- Lambert, G.I., Jennings, S., Hinz, H., Murray, L.G., Lael, P., Kaiser, M.J., Hiddink, J.G., 2013. A comparison of two techniques for the rapid assessment of marine habitat complexity. *Methods Ecol. Evol.* 4, 226–235.
- Legendre, P., Anderson, M.J., 1999. Distance-based redundancy analysis: testing multispecies responses in multifactorial ecological experiments. *Ecol. Monogr.* 69, 1–24.
- Levin, S., 1999. Fragile Dominion. Perseus Publishing, Cambridge, United Kingdom.
- Luckhurst, B.E., Luckhurst, K., 1978. Analysis of influence of substrate variables on coral-reef fish communities. *Mar. Biol.* 49, 317–323.
- McArthur, M.A., Brooke, B.P., Przeslawski, R., Ryan, D.A., Lucieer, V.L., Nichol, S., McCallum, A.W., Mellin, C., Cresswell, I.D., Radke, L.C., 2010. On the use of abiotic surrogates to describe marine benthic biodiversity. *Estuar. Coast. Shelf Sci.* 88, 21–32.
- McCann, K.S., 2000. The diversity–stability debate. *Nature* 405, 228–233.
- Mellin, C., Bradshaw, C.J.A., Fordham, D.A., Caley, M.J., 2014. Strong but opposing beta-diversity–stability relationships in coral reef fish communities. *Proc. R. Soc. B: Biol. Sci.* 281.
- Mellin, C., Delean, S., Caley, J., Edgar, G., Meekan, M., Pitcher, R., Przeslawski, R., Williams, A., Bradshaw, C.J.A., 2011. Effectiveness of biological surrogates for predicting patterns of marine biodiversity: a global meta-analysis. *PLoS ONE* 6, e20141.
- Mellin, C., Parrott, L., Andréfouët, S., Bradshaw, C.J.A., MacNeil, M.A., Caley, M.J., 2012. Multi-scale marine biodiversity patterns inferred efficiently from habitat image processing. *Ecol. Appl.* 22, 792–803.
- Moffitt, R., Pike, B., Shugart-Schmidt, K., 2015. MPAtlas. [www.mpatlas.org](http://www.mpatlas.org) (accessed 16.02.15).

- Moilanen, A., Wilson, K.A., Possingham, H., 2009. *Spatial Conservation Prioritization: Quantitative Methods and Computational Tools*. Oxford University Press, Oxford.
- Musco, L., Terlizzi, A., Licciano, M., Giangrande, A., 2009. Taxonomic structure and the effectiveness of surrogates in environmental monitoring: a lesson from polychaetes. *Mar. Ecol. Prog. Ser.* 383, 199–210.
- Oksanen, J., Blanchet, F.G., Kindt, R., Legendre, P., Minchin, P.R., O'Hara, R.B., Simpson, G.L., Solymos, P., Stevens, M.H.M., Wagner, H.H., 2013. *vegan: Community Ecology Package*, R package version 2.0-9. [www.CRAN.R-project.org/package=vegan](http://www.CRAN.R-project.org/package=vegan) (accessed 11.07.13).
- Oldeland, J., Wesuls, D., Rocchini, D., Schmidt, M., Jürgens, N., 2010. Does using species abundance data improve estimates of species diversity from remotely sensed spectral heterogeneity? *Ecol. Indic.* 10, 390–396.
- Parrott, L., 2010. Measuring ecological complexity. *Ecol. Indic.* 10, 1069–1076.
- Peres-Neto, P.R., Jackson, D.A., 2001. How well do multivariate data sets match? The advantages of a Procrustean superimposition approach over the Mantel test. *Oecologia* 129, 169–178.
- Poore, G.C.B., Wilson, G.D.F., 1993. Marine species richness. *Nature* 361, 597–598.
- Proulx, R., Parrott, L., 2008. Measures of structural complexity in digital images for monitoring the ecological signature of an old-growth forest ecosystem. *Ecol. Indic.* 8, 270–284.
- Proulx, R., Parrott, L., 2009. Structural complexity in digital images as an ecological indicator for monitoring forest dynamics across scale, space and time. *Ecol. Indic.* 9, 1248–1256.
- Przeslawski, R., Currie, D.R., Sorokin, S.J., Ward, T.M., Althaus, F., Williams, A., 2011. Utility of a spatial habitat classification system as a surrogate of marine benthic community structure for the Australian margin. *ICES J. Mar. Sci.* 68, 1954–1962.
- R Core Team, 2013. *R: A Language and Environment for Statistical Computing*. [www.R-project.org/](http://www.R-project.org/) (accessed 11.07.13).
- Richardson, A.J., Poloczanska, E.S., 2008. Under-resourced, under threat. *Science* 320, 1294–1295.
- Rodrigues, A.S.L., Brooks, T.M., 2007. Shortcuts for biodiversity conservation planning: the effectiveness of surrogates. *Annu. Rev. Ecol. Evol. Syst.* 38, 713–737.
- Shumway, C.A., Hofmann, H.A., Dobberfuhl, A.P., 2007. Quantifying habitat complexity in aquatic ecosystems. *Freshw. Biol.* 52, 1065–1076.
- Shurin, J.B., 2007. How is diversity related to species turnover through time? *Oikos* 116, 957–965.
- Smale, D., Langlois, T., Kendrick, G., Meeuwig, J., Harvey, E., 2011. From fronds to fish: the use of indicators for ecological monitoring in marine benthic ecosystems, with case studies from temperate Western Australia. *Rev. Fish Biol. Fish.* 21, 311–337.
- St-Louis, V., Pidgeon, A.M., Radeloff, V.C., Hawbaker, T.J., Clayton, M.K., 2006. High-resolution image texture as a predictor of bird species richness. *Remote Sens. Environ.* 105, 299–312.
- Thibaut, L.M., Connolly, S.R., Sweatman, H.P.A., 2012. Diversity and stability of herbivorous fishes on coral reefs. *Ecology* 93, 891–901.
- Trygonis, V., Sini, M., 2012. photoQuad: a dedicated seabed image processing software, and a comparative error analysis of four photoquadrat methods. *J. Exp. Mar. Biol. Ecol.* 424, 99–108.
- Wackerbauer, R., Witt, A., Atmanspacher, H., Kurths, J., Scheingraber, H., 1994. A comparative classification of complexity measures. *Chaos Solitons Fractals* 4, 133–173.
- Walker, B.H., 1992. Biodiversity and ecological redundancy. *Conserv. Biol.* 6, 18–23.
- Ward, T.J., Vanderklift, M.A., Nicholls, A.O., Kenchington, R.A., 1999. Selecting marine reserves using habitats and species assemblages as surrogates for biological diversity. *Ecol. Appl.* 9, 691–698.
- Watson, D., Harvey, E., Anderson, M., Kendrick, G., 2005. A comparison of temperate reef fish assemblages recorded by three underwater stereo-video techniques. *Mar. Biol.* 148, 415–425.
- Włodarska-Kowalczyk, M., Kędra, M., 2007. Surrogacy in natural patterns of benthic distribution and diversity: selected taxa versus lower taxonomic resolution. *Mar. Ecol. Prog. Ser.* 351, 53–63.